COMPUTATIONAL STUDY OF RADIATIVE AND CONVECTIVE HEAT TRANSFER IN A CYLINDRICAL COMBUSTION CHAMBER

S. H. Mansouri, M. A. Mehrabian, S. Gallehdari and M. Rahnama

Department of Mechanical Engineering, Shahid Bahonar Kerman University
P. O. Box 76169-133, Kerman, Iran, mansouri@alum.mit.edu

(Received: September 23, 2002 – Accepted in Revised Form: May 15, 2003)

Abstract In this paper, the effect of cold air on the fluid flow inside the cylindrical combustion chamber and its wall temperature distribution have been studied computationally, taking into account the effect of radiative heat transfer from hot gases. The results have been compared with the case that radiative heat transfer was neglected. It is observed that the reattachment length increases when increasing the expansion ratio, and mixing of two fluid flows are not affected by temperature. As mixing is directly related to turbulence, higher turbulence will cause uniform mixture in a shorter length and sudden expansion is helpful for faster mixing. The results show that the combustion chamber wall temperature due to gas radiation will increase very quickly at the entrance and will then decrease rapidly, while neglecting the radiation effect, the wall temperature will increase monotonically.

Key Words CFD, Power Law, Hybrid Schemes, Radiation Heat Transfer, Combustion Chamber

چکیده جریان سیال در بسیاری از فرایندهایی که در محفظه احتراق اتفاق می‌افتند آشفته است. با آگاهی از تاثیر پارامترهای مختلف بر جریان و فرآیندهای انتقال حرارت می توان طراحی محفظه احتراق را بهینه کرد. در این مقاله تاثیر هوای سرد بر جریان سیال در داخل محفظه احتراق استوانه ای شکل و توزیع درجه حرارت در دیوارهٔ آن مورد مطالعه قرار گرفته است. در این مطالعه اثر انتقال حرارت تابشی از گازهای داغ منظور شده است. نتایج حاصله از این کار با نتایج بدست آمده بدون در نظر گرفتن انتقال حرارت تابشی مقایسه گردیده است. معادلات جرم، اندازه حرکت و انرژی در حالت های آرام و آشفته با استفاده از روش حجم محدود و طرح توانی منفصل شده اند. معادلات منفصل شده با استفاده از آلگوریتم سیمپلر بطور عددی حل شده اند. ملاحظه می شود که با افزایش نسبت انبساط فاصله گرداب ها افزایش می یابد، ضمناً اختلاط دو جریان سیال متاثر از درجه حرارت نیست. با توجه به اینکه اختلاط با آشفتگی رابطه مستقیم دارد، آشفتگی شدیدتر باعث می شود که مخلوط یکنواخت در فاصله کوتاهتری حاصل شود. ضمناً انبساط شدید در سرعت اختلاط موثر است. نتایج حاصل نشان میدهند که درجه حرارت دیواره محفظه احتراق در مدخل محفظه بر اثر تابش گازی سریعاً افزایش و سپس کاهش می یابد. این در حالی است که بدون در نظر گرفتن اثر تابش، درجه حرارت دیواره بطور یکنواخت افزایش می‌یابد.

1. INTRODUCTION

Combustion chamber design is of great importance. The geometry of these chambers may change gradually or suddenly. When the fluid path changes abruptly, flow parameters, flow characteristics, and the heat transfer will change. Knowing how the flow parameters, the flow characteristics, and the heat transfer rate change in these chambers enables the engineer to optimise his design. In boilers, furnaces, internal combustion engines, and surfaces exposed to direct gas radiation, the dominant mode of heat transfer is radiation.

In order to control the temperature rise in such devices a cooling system should be supplied. Temperature control in the combustion chamber walls, the turbine internal space, the exit of convergent nozzle, and also in the burners with continuous combustion is specifically important because of metallurgical limitations. Because of limitations in flammability in such devices, the fuel-air ratio cannot be lower than a certain value. The temperature of the products varies with pressure and fuel-air ratio. The operating temperature is usually more than the allowable temperature for the wall. Reducing the wall temperature by transpiration cooling provides excess air to the combustion chamber. In most designs, the excess air enters through the sidewalls.

Forced convection combined with radiation in

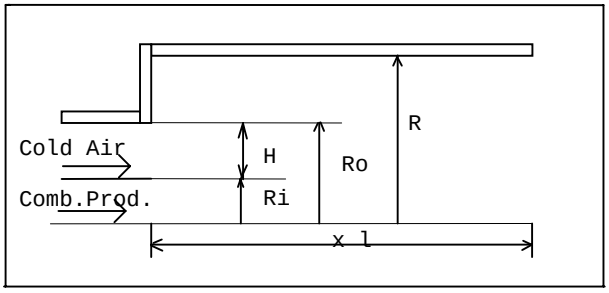

Figure 1. Flow geometry and solution domain.

the developed region inside a channel with horizontal plates is given by dimensionless equations and using a two layer model to simulate the turbulence [1]. A numerical procedure has been applied to study the convection and radiation heat transfer in channels with rectangular and triangular cross sections in laminar flow [2]. Nisbet et al. [3] presented a summary of recent works in turbulent flow. In this summary, the details of experimental and numerical methods and also the turbulence modeling procedures have been outlined. Ohtsuka [4] has performed a numerical study for the flow inside the combustion chamber. The fuel and air enter the cylindrical chamber with a sudden expansion. Fuel and air enter as two horizontal streams. Two different models for combustion and three different models for turbulence have been studied. The results were presented as velocity and temperature profiles and also velocity distribution along the chamber axis. These results were compared with experimental data [11,14]. The numerical study of reactive and non-reactive flows have been performed using the Reynolds stress differential model. The mixing of air and helium and the combustion of air and propane have both been modeled [5].

Radiative heat transfer in combustion chambers and furnaces has been studied in details [15]. Statistical models have been presented for gas radiation [16]. An exact numerical procedure has been developed to solve radiative heat transfer in cylindrical furnaces [18]. A comparative study has been carried out to evaluate the radiative heat transfer models in furnaces [18]. Furnace heat transfer processes have been studied numerically [19, 20]. In this study, the processes involved in a cylindrical furnace have been modeled by one dimensional, time dependent equations. These equations present satisfactory results. The temperature distribution in a three-zone furnace has been simulated [21]. A comprehensive study about heat transfer in industrial furnaces has been reported [22, 23]. In this report, the model equations for flame furnaces are presented, and the contribution of different heat transfer modes in the total furnace heat transfer are established. High temperature furnaces have been modeled [24].

In the present study, it is assumed that the excess air enters the cylindrical combustion chamber through an annular path. The cold excess air covers the combustion products and acts as a protecting layer to control the combustion chamber wall temperature. In this paper, parametric study of the flow field, heat transfer and mixing of two fluids in turbulent flow are studied. The effect of gas radiation and turbulent mixing of cold air on the flow inside the combustion chamber are considered. The parametric investigation to study the effect of injection height on flow, heat transfer and fuel-air ratio is also presented.

Liakos, H. H., et al, 2000 [25] presented a two-dimensional model simulating the combustion characteristics of a non-premixed natural gas flame under high strain using the same principles. The model takes account of the turbulent flow characteristics, the reaction rates controlled by mixing and chemical kinetics mechanisms and heat transfer with convection and radiation. Three turbulence models, two two-equation models and one second order, were assessed and evaluated with respect to accurate prediction of the turbulent characteristics of the flame. The mechanisms that control the combustion phenomenon were analyzed. The computational results were compared with experimental data with satisfactory agreement.

2. GOVERNING EQUATIONS

The governing equations and boundary conditions, the flow geometry and the solution domain are shown in Figure 1 As the figure shows, one half of the combustion chamber is considered as the solution domain. The governing equations for two dimensional laminar and turbulent compressible flow are considered. In these equations j is zero for two-dimensional flow and one for axisymmetrical flow. The standard k-ε turbulence model is used to simulate the Reynolds stresses [1,3,10].

a) The Continuity Equation:

$$\frac{\partial}{\partial x}(\rho u)+\frac{1}{r^j}\frac{\partial}{\partial r}(r^j\rho v)=0 \tag{1}$$

b) The Momentum Equation:
Axial component:

$$\frac{\partial}{\partial x}\left(\rho u^2\right)+\frac{1}{r^j}\frac{\partial}{\partial r}\left(r^j\rho uv\right)=$$
$$\frac{\partial}{\partial x}\left(\mu_{eff}\frac{\partial u}{\partial x}\right)+\frac{1}{r^j}\frac{\partial}{\partial r}\left(r^j\mu_{eff}\frac{\partial u}{\partial r}\right)+s_u \tag{2}$$

where,

$$s_u \equiv -\frac{\partial P}{\partial x}+\frac{\partial}{\partial x}\left(\mu_{eff}\frac{\partial u}{\partial x}\right)+\frac{1}{r^j}\frac{\partial}{\partial r}\left(r^j\mu_{eff}\frac{\partial v}{\partial x}\right)-$$
$$\frac{2}{3}\frac{\partial}{\partial x}(\rho k)-\frac{2}{3}\frac{\partial}{\partial x}\left[\mu_{eff}\frac{\partial u}{\partial x}+\mu_{eff}\frac{1}{r^j}\frac{\partial}{\partial r}\left(r^j v\right)\right] \tag{3}$$

and radial component:

$$\frac{\partial}{\partial x}(\rho uv)+\frac{1}{r^j}\frac{\partial}{\partial r}\left(r^j\rho v^2\right)=$$
$$\frac{\partial}{\partial x}\left(\mu_{eff}\frac{\partial v}{\partial x}\right)+\frac{1}{r^j}\frac{\partial}{\partial r}\left(r^j\mu_{eff}\frac{\partial v}{\partial r}\right)+s_v \tag{4}$$

where,

$$s_v \equiv -\frac{\partial P}{\partial r}+\frac{\partial}{\partial x}\left(\mu_{eff}\frac{\partial u}{\partial r}\right)+\frac{1}{r^j}\frac{\partial}{\partial r}\left(r^j\mu_{eff}\frac{\partial v}{\partial r}\right)$$
$$-2\mu_{eff}\frac{jv}{r^2}-\frac{2}{3}\frac{1}{r^j}\frac{\partial}{\partial r}\left[\mu_{eff}\left(\frac{\partial u}{\partial x}+\frac{1}{r^j}\frac{\partial}{\partial r}\left(r^j v\right)\right)+r^j\rho k\right]$$
$$+\frac{2}{3}\frac{1}{r^j}\left[\rho k+\mu_{eff}\left(\frac{\partial u}{\partial x}+\frac{1}{r^j}\frac{\partial}{\partial r}\left(r^j v\right)\right)\right] \tag{5}$$

c) Scalar Equations:

The variables k, ε, T and w satisfy the following equations:

$$\frac{\partial}{\partial x}(\rho u\phi)+\frac{1}{r^j}\frac{\partial}{\partial r}\left(r^j\rho v\phi\right)=$$
$$\frac{\partial}{\partial x}\left(\Gamma_{eff}\frac{\partial\phi}{\partial x}\right)+\frac{1}{r^j}\frac{\partial}{\partial r}\left(r^j\Gamma_{eff}\frac{\partial\phi}{\partial r}\right)+s_\phi \tag{6}$$

in which,

$$\Gamma_{eff}\equiv\frac{\mu_{eff}}{\sigma_\phi} \tag{7}$$

The source term for w is zero and for T, k and ε are as follows:

$$\phi\equiv T \quad , \quad S_T\equiv -\operatorname{div}q_r$$
$$\operatorname{div}q_r=-\frac{k_a}{C_P}\left(G-4\sigma T^4\right) \tag{8}$$

variable G satisfies the following equation:

$$\frac{\partial^2 G}{\partial x^2}+\frac{1}{r}\frac{\partial}{\partial r^j}\left(r^j\frac{\partial G}{\partial r}\right)=3\beta k_a(G-4\sigma T^4) \tag{9}$$

The gradient of thermal radiation on the wall satisfies the following equation:

$$\frac{\partial G}{\partial r}=-\frac{3}{2R}\frac{\varepsilon_w}{2-\varepsilon_w}\tau_R\left(G-4\sigma T_w^4\right) \tag{10}$$

$$\phi\equiv k \quad , \quad S_k\equiv P-\rho\varepsilon \tag{11}$$

$$\phi\equiv\varepsilon \quad , \quad S_\varepsilon\equiv C_1 P\frac{\varepsilon}{k}-C_2\,\rho\frac{\varepsilon^2}{k} \tag{12}$$

$$P=2\mu_{eff}\left[\left(\frac{\partial u}{\partial x}\right)^2+\left(\frac{\partial v}{\partial r}\right)^2+j\left(\frac{v}{r}\right)^2\right]+\mu_t\left(\frac{\partial u}{\partial r}+\frac{\partial v}{\partial x}\right)^2 \tag{13}$$

where,

$$\mu_{eff}=\mu+\mu_t,\quad \mu_t=C_\mu\rho k^2/\varepsilon \tag{14}$$

The constants for the turbulence model are as follows:

$$C_1 = 1.44 \ , \ C_2 = 1.92 \ , \ C_\mu = 0.09 \ , \ \ \sigma_K = 1.0 \ , \ \sigma_\varepsilon = 1.3 \tag{15}$$

$$\phi \equiv w \qquad , \qquad S_w \equiv 0 \tag{16}$$

The properties of the mixture are calculated using Refs. [7, 8 & 9].

d) Boundary Conditions The no slip condition (zero velocity) on the solid surface has been applied. Two steady state flows with different velocities have been considered at the chamber's entrance. The entrance velocity for each flow in the x-direction is $u = u_i$ and the exit velocity is $u = u_o$. The entrance velocity in the r-direction is zero. The exit velocity in the x direction is corrected using the mass balance equation in each iteration. The difference between the entrance and exit masses is divided by the product of density and combustion chamber's cross sectional area. The result is an average velocity that is added to the previous velocity and is considered as the exit velocity. The symmetry condition is applied on the lower boundary. The wall function is used for the velocity near the boundary:

$$\mu_{eff_{atwall}} = \begin{cases} \mu & y^+ < 11.5 \\ \dfrac{\mu y^+}{2.5 \ln(9y^+)} & y^+ \geq 11.5 \end{cases} \tag{17}$$

where

$$y^+ \equiv \rho k^{1/2} C_\mu^{1/4} y_p / \mu \tag{18}$$

The solid wall is either adiabatic or isothermal (temperature boundary condition). The entrance and exit temperatures are variable and considered as $T = T_i$ and $T = T_o$ respectively. The symmetry applies on the lower boundary. When the solid boundary's temperature is constant the wall function used for temperature is as follows:

$$\frac{\mu_{eff_{atwall}}}{\sigma_t} = \begin{cases} \dfrac{\mu}{\sigma_t} & y^+ < 11.5 \\ \dfrac{\mu y^+}{\sigma_t \left[2.5 \ln(9y^+) + 9\left(\dfrac{\sigma}{\sigma_t} - 1\right)\left(\dfrac{\sigma}{\sigma_t}\right)^{-1/4} \right]} & y^+ \geq 11.5 \end{cases} \tag{19}$$

in which σ and σ_t are the laminar and turbulent Prandtl numbers respectively. If the solid wall is adiabatic the following condition is applied on the wall:

$$\frac{\partial T}{\partial r} = 0 \tag{20}$$

It is assumed that the production and dissipation of kinetic energy at the vicinity of solid boundaries are equal. These values at the entrance are as follows:

$$\begin{aligned} k &= 0.005 \times u_{in}^{\ 2} \\ \varepsilon &= 0.1 \times k^2 \end{aligned} \tag{21}$$

The gradients of k and ε at the exit are zero. Two boundary conditions are considered for the mass fraction at the entrance, one for the inner flow and zero for the outer flow. The mass fraction gradient at the exit in the x-direction is zero and symmetrical velocities are applied on the lower boundary.

3. NUMERICAL SOLUTION

The finite volume method and power law scheme have been used to transform the partial differential equations into finite difference algebraic equations. The computational domain has been considered as a Cartesian mesh that covers the whole solution domain. The displaced mesh has been used to discrete the pressure gradient and velocity in momentum and continuity equations. The unsteady mesh has been enlarged in the x-direction. The properties of mixture change with respect to temperature, pressure and mass fraction. Therefore, the equations are coupled and should be solved simultaneously. The unknown term (pressure) in the momentum equation is found using the SIMPLER

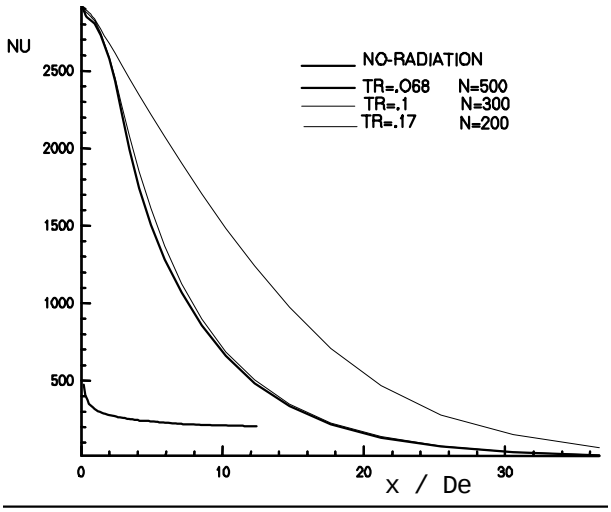

Figure 2. Effect of optical thickness on local Nusselt number.

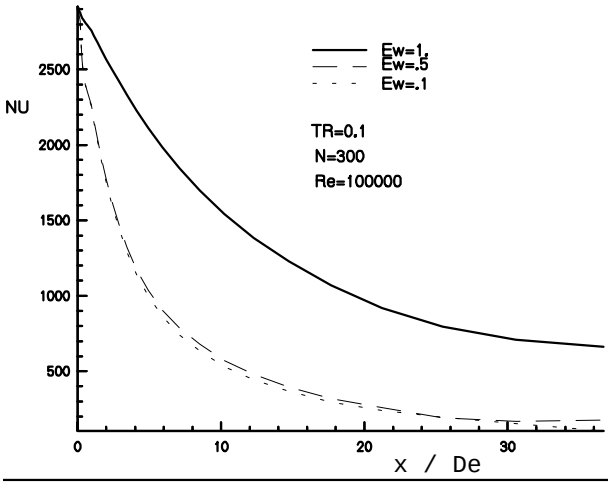

Figure 3. Effect of emissivity on local Nusselt number.

algorithm so that the continuity equation is satisfied.

The convergence criterion has been chosen in such a way that the sum of momentum and mass residuals is less than 0.001. In order to prevent the non-linear equations from diverging, the under relaxation coefficient of 0.7 is used for velocity, 1 for pressure, 0.8 for temperature and mass fraction and 0.6 for production and dissipation of turbulence kinetic energy.

4. RESULTS AND DISCUSSION

a) Sensitivity Analysis and Accuracy Accuracy studies and sensitivity analysis of air in a channel with a sudden expansion, without injecting excess air and together with radiation at different expansion ratios have been investigated by S. Gallehdari [14]. There is good agreement between experimental and numerical results [11]. To obtain the optimal number of grid points, sensitivity analysis has been taken into account: the numerical results have been obtained using three different mesh sizes, namely 40x20, 60x30 and 80x40. It has been noticed that the grid independent solution is obtained for the 60x30. The grids finer than that do not alter the accuracy of numerical results. The numbers of iterations that lead to the grid independent solution varies with the Reynolds number at the inlet.

b) Gas radiation effects The effects of optical thickness and emissivity on the local Nusselt number for the turbulent flow between two parallel plates when Re = 100,000 are shown in Figures 2 and 3. The figures show that the local Nusselt number increases with optical thickness as well as with gas emissivity.

The dimensionless temperature at the wall for two fluids at different temperatures is illustrated in Figure 4 when H/R=1.5. In Figure 5 the dimensionless temperature at the wall for two fluids at the same temperature is shown in a sudden expansion together with radiation. It can be concluded that the radiation at the combustion chamber's entrance is very effective and may raise the wall temperature considerably. In practice, we may use thermal shield or any other technique in order to prevent the wall temperature exceeding a certain limit. Figure 5 shows the temperature distribution near the wall for two fluids at different temperatures in a sudden expansion with radiation effects.

c) Mixing Effects To study the effect of mixing, a combustion chamber, 0.10m in diameter and 2.5m long, is considered. It is assumed that the combustion products at 1000 K and 0.005 kg/s enter the combustion chamber. Making the mass flow of hot and cold fluids constant, the inlet flow velocities will change with the inlet height, H.

A typical flow field for H/R=0.4 is illustrated in Fig. 6. The rotational region on the centreline and the developing flow field along the chamber are high-lighted in the figure. In Fig. 7 the streamlines are drawn for three different H/R ratios. The rotational

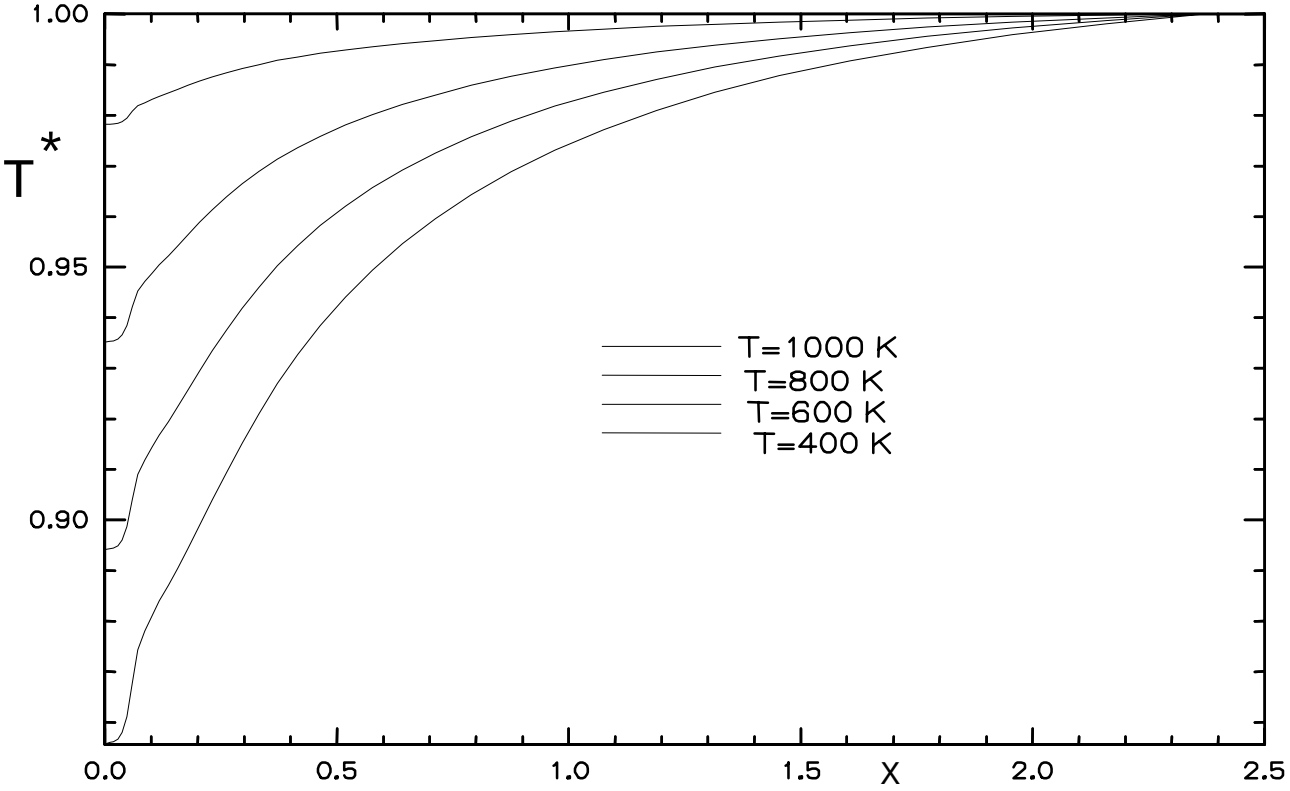

Figure 4. Temperature distribution near the wall for two fluids at the same temperature.

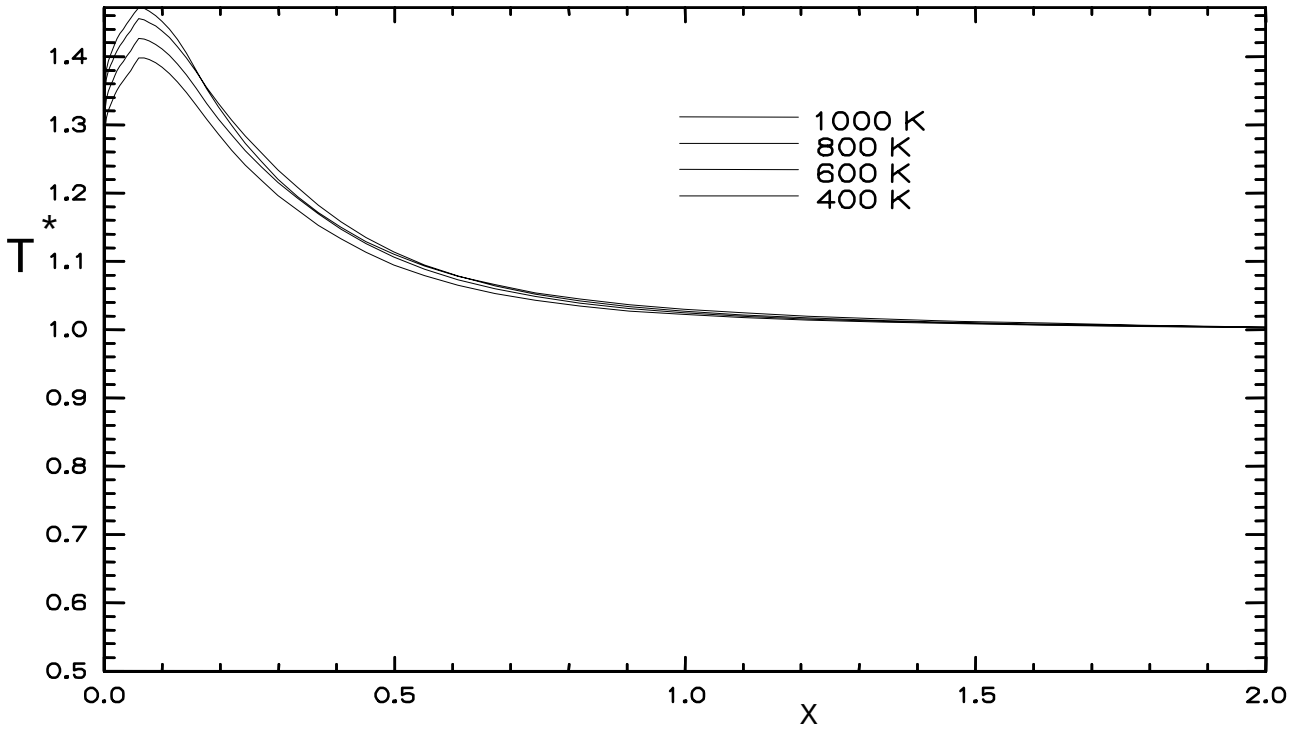

Figure 5. Temperature distribution near the wall for two fluids at different temperatures.

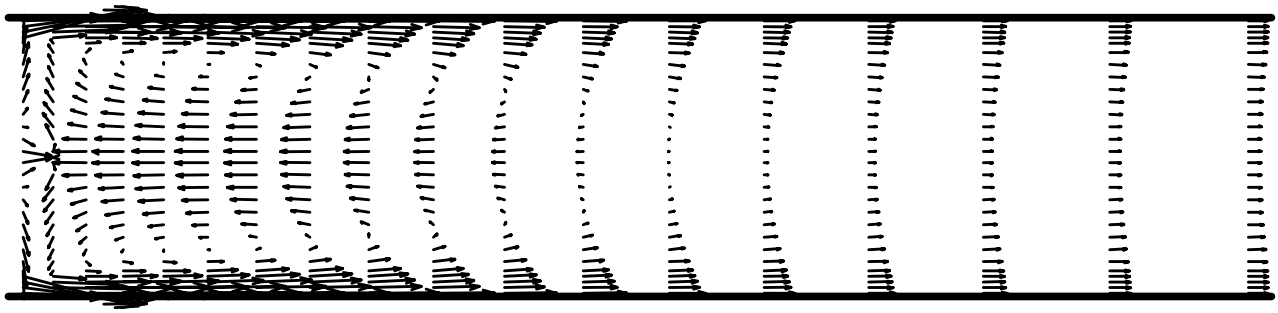

Figure 6. Turbulent flow field for two fluids in the combustion chamber.

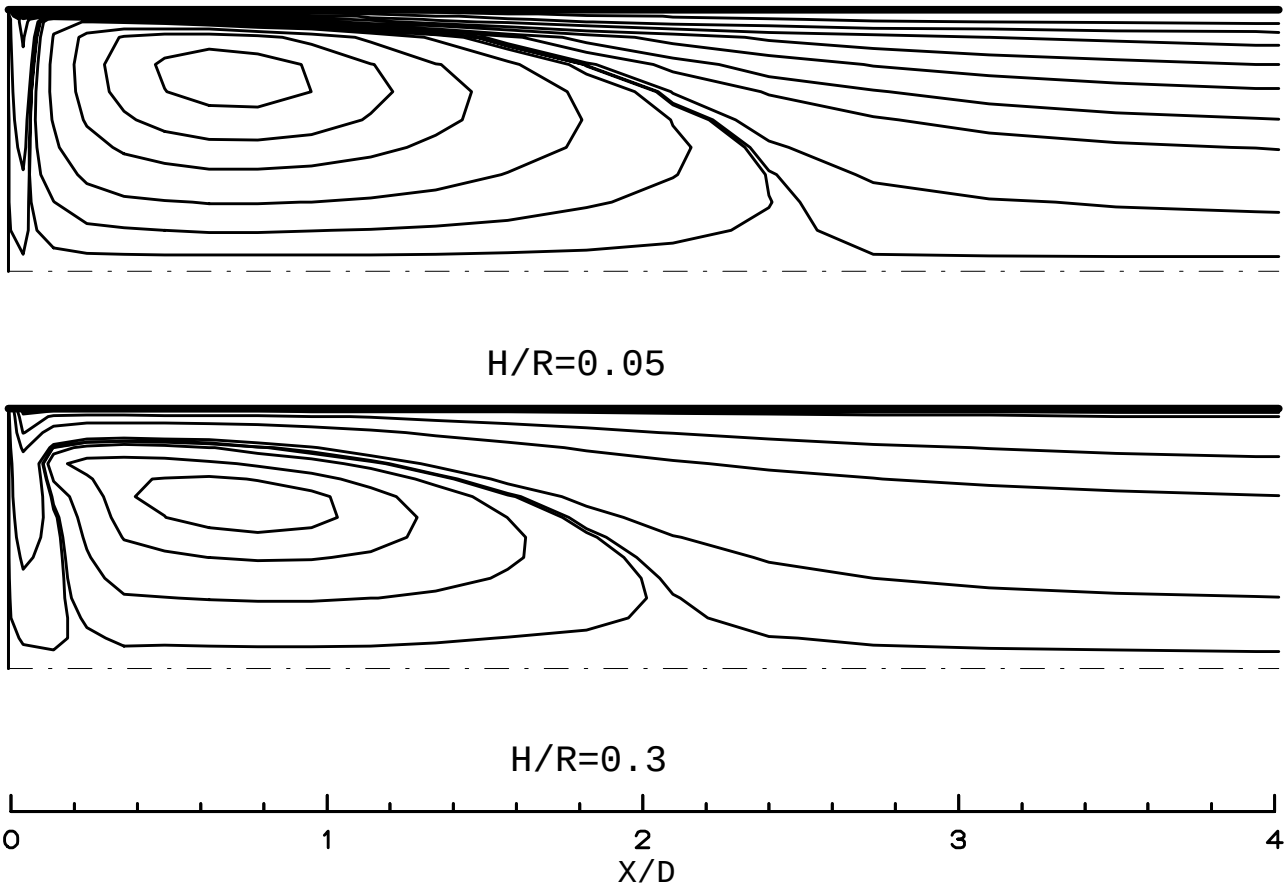

Figure 7. Streamlines for mixing of two fluids at different H/R ratios.

region on the centerline which is formed as a result of different flow velocities is shown in the figure. The length and height of the rotational region decrease as the H/R increases. The starting point of the rotational region is also shifted to a further distance from the inlet section. The bigger the rotational region, the better the mixing process and the sooner the homogenous mixture is formed.

In Figures 8 and 9 the lines of constant temperature and constant mass fraction ratio are shown respectively. It can be seen that the shape of the above lines are almost similar. This is because

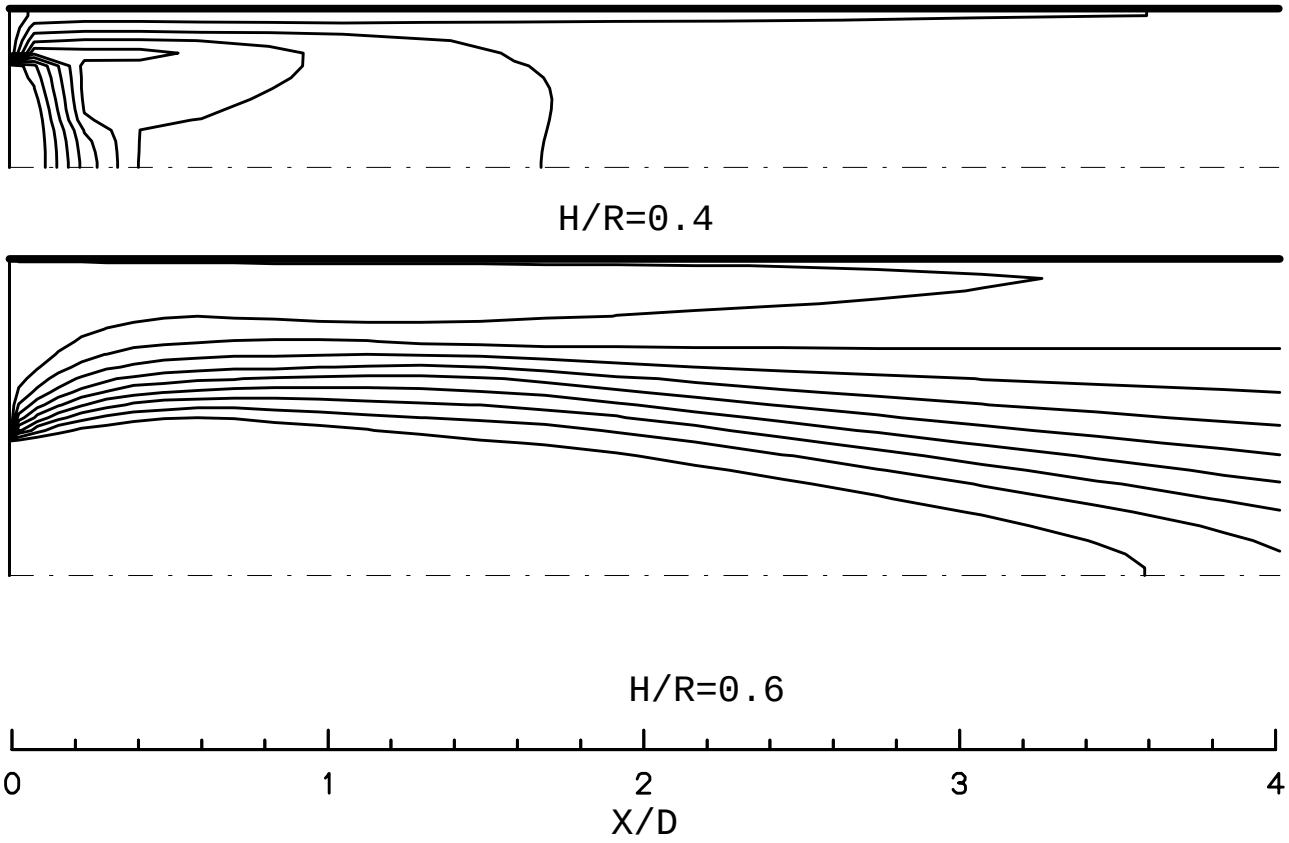

Figure 8. Temperature contours for mixing of two fluids at different H/R ratios.

of the similarity in differential equations and boundary conditions applied for temperature and mass fraction ratio. In fact, when Pr=Sc, the dimensionless equations for mass fraction and temperature are the same. In Figure 10 the lines of constant k are drawn for H/R=0.05 and H/R=0.5. It can be seen that the lower the H/R the higher the kinetic energy. The ratios of turbulent kinetic energy for the above ratios are 75 to 1. As a result, it is realized that mixing process is directly related to turbulence. That means for the higher degrees of turbulence the mixing process is accomplished faster. The other statement from the above figures is that at low H/R ratios, as a result of rotational region on the centerline, the cold fluid diffuses into the hot fluid while at high H/R ratios the direction of diffusion is reversed. The variation of mass fraction ratio along the combustion chamber using power law and hybrid schemes at four different temperatures is illustrated in Figures 11 and 12. As can be seen from the above figures, increasing the temperature does not affect the mixing process. In Figure 13 a typical flow field in the combustion chamber with a sudden expansion is illustrated. The streamlines are shown for expansion ratios of 1.5, 2 and 3 in Figure 13. The figure shows the bigger the expansion ratio, the longer the rotational region.

In order to study the effect of sudden expansion on fluids mixing, the expansion ratio and the fluid mass flow rate are assumed to be 1.5 and 50 g/s respectively. The typical flow field is shown in Figure 14. This figure indicates the velocity vectors in the rotational regions produced behind the inlet expansion along the centerline. Figure 14 indicates the streamlines when H/R is 0.1, 0.3 and 0.45. As the figure shows, two rotational regions are created, one behind the expansion and the other one along the centerline. The dimensions of rotational region along the centerline decrease and its starting point gets further from the inlet region when H/R increases. The lines of constant temperature and mass

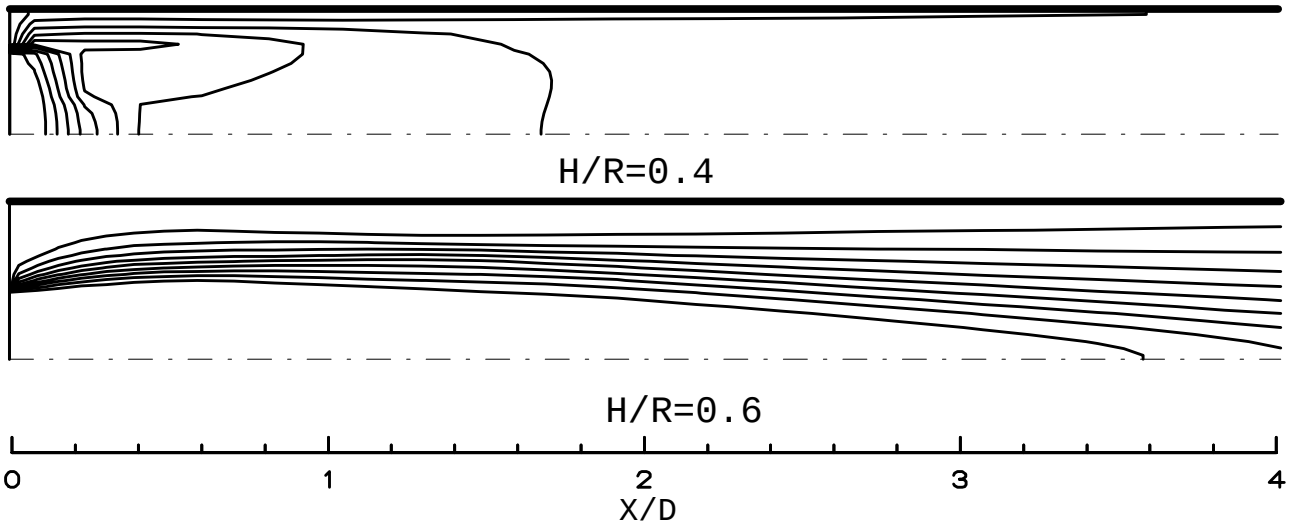

Figure 9. Mass fraction contours for mixing of two fluids at different H/R ratios.

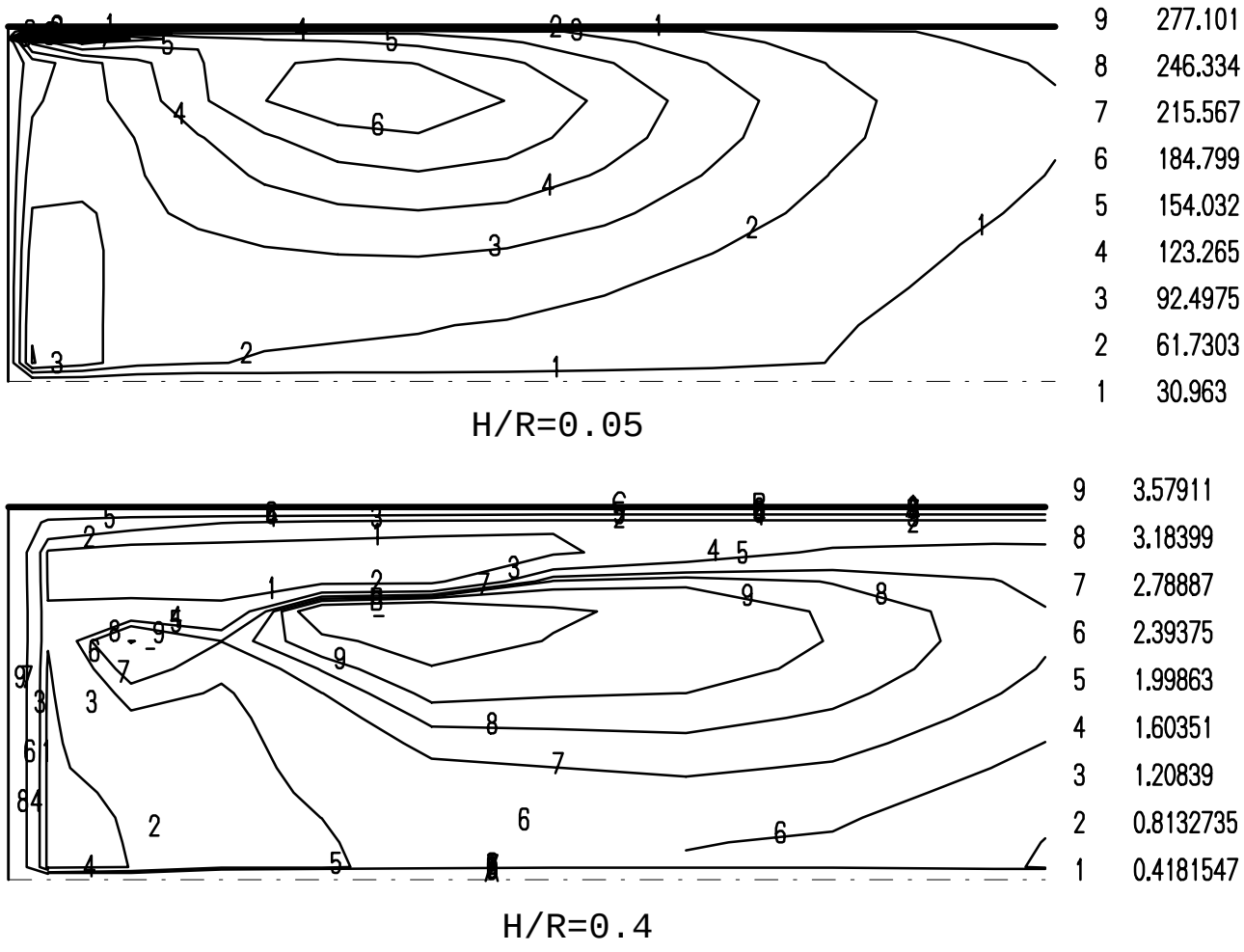

Figure 10. Comparison of energy contours at two different H/R ratios.

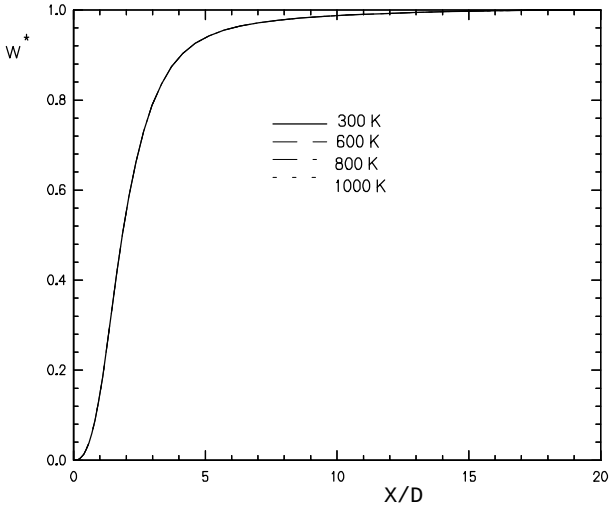

Figure 11. Mass fraction distribution near the wall for two fluids.

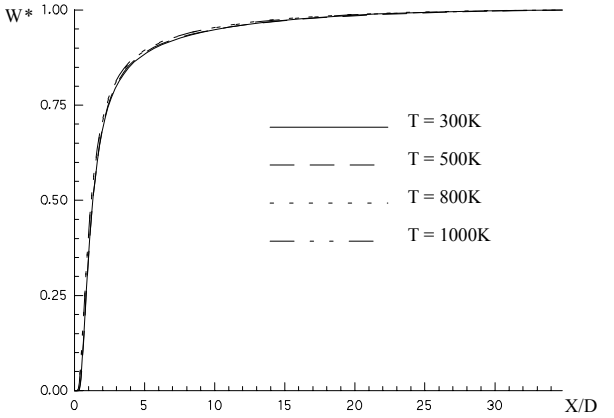

Figure 12. Mass fraction distribution near the wall for two fluids at different temperatures.

ratio are indicated in Figure 15. This figure shows that the mass diffusion rate is higher and the mixing process is performed more rapidly as a result of sudden expansion, in other words, a more uniform mixture is produced at a shorter distance.

d) Comparison with experimental data

Experimental data are available [25] for temperature distribution along the center-line of a cylindrical combustion chamber having the aspect ratio of 3.38, the fuel inlet, primary air and secondary air temperatures of 295 K. The combustion chamber being studied in this paper has an aspect ratio greater than 10, so that thermally developed turbulent regime is ensured.

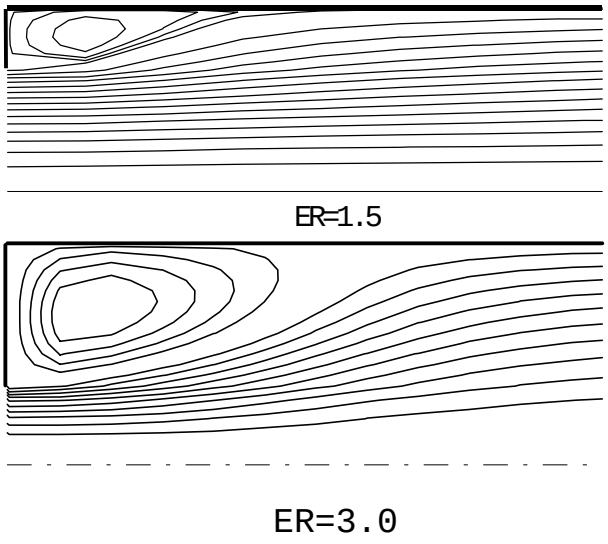

Figure 13. Streamlines for turbulent flow for different ER.

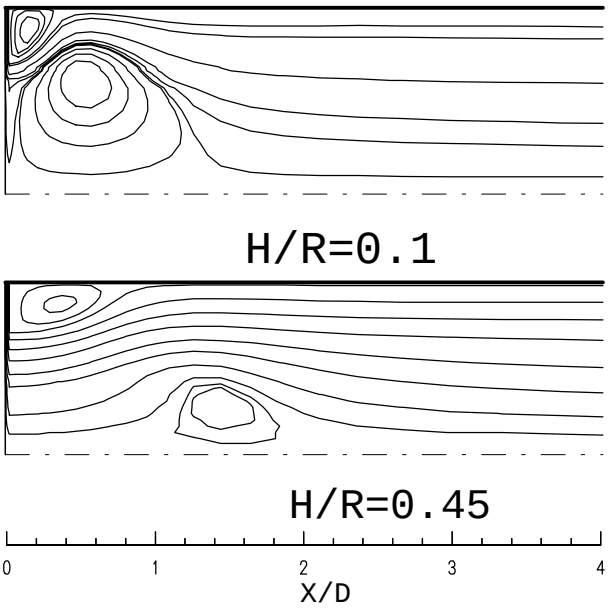

Figure 14. Streamlines for mixing of cold and hot fluids.

5. CONCLUSIONS

Fluid flows in many processes taking place in combustion chamber are turbulent. Combustion

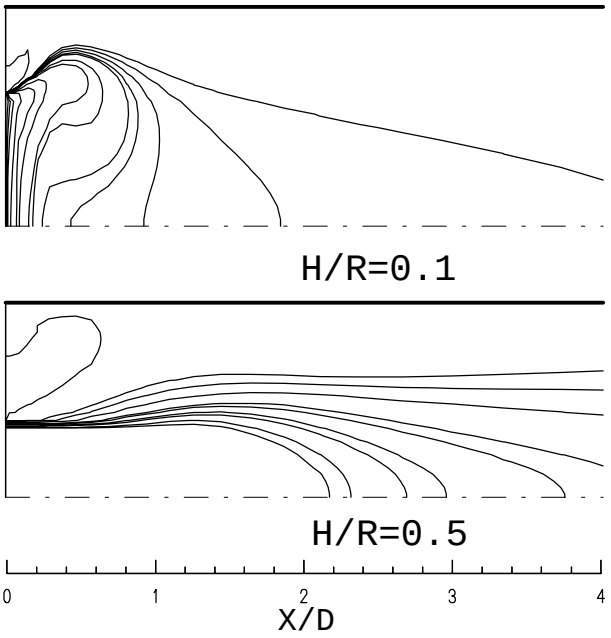

Figure 15. Contours of mass fraction.

chamber can be designed optimally by knowing the effect of different parameters on the flow and heat transfer processes that are involved. The mass, momentum and energy equations for the laminar and turbulent cases were solved computationally using a finite volume approach and power law scheme. Semi-Implicit Method for Pressure Linked Equations Revised (SIMPLER) algorithm was used in the computational procedure.

The numerical modeling and parametric study were carried out to investigate the effect of injecting height of the cold air on fluid flow, heat transfer and mass fraction ratio of two fluids in the mixture. The study indicates that the temperature difference is not an important parameter on the mass fraction. Furthermore, the variation of mass fraction of two fluids is directly related to the degree of turbulence. It is also evident that higher turbulence, results in more uniform mixtures at shorter distances. The study reveals that the higher the injecting point, the lower the mean and the maximum temperature of combustion chamber. It is also clear that the local Nusselt number increases with emissivity and the optical thickness of the gas. It also increases as the conduction-radiation parameter decreases.

The effect of radiation on the Nusselt number at the inlet is very important. A comparison between the without-radiation and with-radiation cases can be made in Figure 2, which shows the Nusselt number at the entrance with-radiation is about 6 times bigger than that without-radiation. This ratio decreases along the positive x-axis and approaches one at the exit of combustion chamber.

The effect of emissivity on the Nusselt number at outlet of combustion chamber is significant. A comparison is made in Figure 3, where the local Nusselt number is shown for three different emissivities . The Nusselt number at exit for $\varepsilon=1$ is almost 6 times bigger than that for $\varepsilon=0.5$. This ratio decreases along the negative x-axis and approaches one at the inlet.

Thus, considering the operating conditions, the optimum values for the parameters involved in combustion chamber design can be selected using parametric studies.

6. ACKNOWLEDGMENT

The study was partly supported by the International Center for Science, High Technology and Environmental Sciences, Kerman, Iran.

7. NOTATION

C_1, C_2, C_μ	Turbulence model constants
C_p	Specific heat at constant pressure
D	Combustion chamber diameter
G	Total radiation
$H = R_o - R_i$	Height of outer flow
k	Turbulent kinetic energy
k_a	Overall absorption coefficient
M	Molecular weight
N	Conduction-radiation parameter
Nu	Nusselt number
P	Pressure, turbulent kinetic energy production rate
Pr	Prandtl number
R	Combustion chamber radius
Re	Reynolds number
R_i	Internal radius
R_o	External radius

Sc	Schmidt number
T	Temperature
w	Mass fraction
u , v	Velocity components
x , r	Coordinate directions
x_l	Length of combustion chamber

Greek Symbols

β	Extinction coefficient
ρ	Density
μ	Dynamic viscosity
μ_t	Turbulent viscosity
μ_{eff}	Effective viscosity
ε	Turbulent energy dissipation rate
σ	Laminar Prandtl number
σ_t	Turbulent Prandtl number
σ_k	Turbulence model constant
σ_ε	Turbulence model constant
ε_w	Wall emissivity
τ_R	Optical thickness, $\tau_R = k_a R$

8. REFERENCES

1. Launder, B. E., "On The Computation of Convective Heat Transfer in Complex Turbulent Flows", ***Journal of Heat Transfer***, Vol. 110, (1988), 1112-1128.
2. Pletcher, R. H., "Progress in Turbulent Forced Convection", ***ASME Journal of Heat Transfer***, Vol. 110, 1988, 1129-1144.
3. Nisbet, J., Davidson, L. and Olsson, E., "Analysis of Two Fast-Chemistry Combustion and Turbulence Modeling in Variable Density Flow", ***Computational Fluid Dynamics Conf.***, Vol. 1, (1992), 557-563.
4. Ohtsuka, M., "Numerical Analysis of Swirling Non-Reacting and Reacting Flows by The Reynolds Stress Differential Method", ***Int. J. Heat Mass Transfer.***, Vol. 38, (1995), 331-337.
5. Anderson, D. A., Tannehil, J. C. and Pletcher, R. H., "Computational Fluid Mechnics and Heat Transfer", Hemisphere, Pub. Cor., (1984).
6. Jayatilleke, C. L. V., "The Influence of Prandtl Number and Surface Roughness on the Resistance of the Laminar Sublayer to Momentum and Heat Transfer", ***Progr. Heat Mass Transfer***, Vol. 1, (1969), 193-329.
7. Reid, R. C., Pruosnit, J. M. and Ploing, B. E., "The Properties of Gases and Liquids", 4th. ed., McGrow - Hill, New York, (1987).
8. Mansouri, S. H. and Heywood, J. B., "Correlations for Viscosity and Prandtl Number of Hydrocarbon-Air Combustion Products", ***Combust. Sci. Technology***, Vol. 23, (1980), 251-256.
9. Heywood, J. B., "Internal Combustion Engine Fundamentals", McGraw-Hill Book Co., (1988).
10. Patankar, S. V., "Numerical Heat Transfer and Fluid Flow", Hemisphere Publishing Corporation, U.S.A., (1980)
11. Yener, Y., Ozisik, M. N., "Simultaneous Radiation and Forced Convection in Thermally Developing Turbulent Flow Through a Parallel-Plate Channel", ***ASME Journal of Heat Transfer***, Vol. 108, (1986), 985-988.
12. Schuler, C. and Campo, A., "Numerical Prediction of Turbulent Heat Transfer in Gas Pipe Flow Subject to Combined Convection and Radiation", ***Int. J. Heat and Fluid Flow***, Vol. 9, (1988), 308 - 315.
13. Siegel, R. and Howell, J. R., "Thermal Radiation Heat Transfer", 3rd. ed., McGraw-Hill Book Company, New York, (1992).
14. Gallehdari, S., "Numerical Investigation of Combined Radiation and Convection Heat Transfer and Turbulent Mixing of Two Fluids in Ducts", ***M.Sc. Thesis***, Dept. of Mechanical Eng., Kerman University, April (1998).
15. Sparrow, E. M. and Cess, R. D., "Radiation Heat Transfer", Hemisphere Publishing Corp., New York, (1978).
16. Liu, Gulder, O. L. and Smallwood, G. J., "Non-Gray Gas Radiative Transfer Analysis Using Statistical Narrow-Band Model", ***Int. J. Heat Mass Transfer***, Vol. 41, No. 14, (1998), 2227-2236.
17. Selcuk and Tahiroglu, Z., "Exact Numerical Solutions for Radiative Heat Transfer in Cylindrical Furnaces", ***Int. J. Numerical Methods in Engineering***, Vol. 26, (1988), 1201-1212.
18. Liu, Becker, H. A. and Bindar, Y., "A Comparative Study of Radiative Heat Transfer Modelling in Gas-fired Furnaces Using the Simple Gray Gas and the weighted Sum-of-Gray-Gases Models", ***Int. J. Heat Mass Transfer***, Vol. 41, (1998), 3357-3371.
19. Jaluria, Y., "Numerical Study of the Thermal Processes in a Furnace", ***Numerical Heat Transfer***, Vol. 7, (1984), 211-224.
20. Jaluria, Y., "Numerical Simulation of the Transport Processes in a Heat Treatment Furnace", ***Int. J. Numerical Methods in Engineering***, Vol. 25, (1988), 387-399.
21. Boschert, St., Dold, P. and Benz, K. W., "Modelling of the Temperature Distribution in a Three-Zone Resistance Furnace Configuration and Ampule Position", ***J. Crystal Growth***, Vol. 187, (1998), 140-149.
22. Chapman, Ramadhyani, S., Ramamurthy, H. and Viscanta R., "Heat Transfer in Industrial Furnaces", Annual Report, Gas Research Institute, (1991).
23. Chapman, Ramadhyani, S., Ramamurthy, H. and Viscanta R., "Heat Transfer in Industrial Furnaces", Annual Report, Gas Research Institute, (1992).
24. Smith, "High Temperature Furnace Modelling and Performance Verification", Technical Report, Dept. of Chemical and Materials Engineering, University of Alabama, (1992).
25. Liakos, H. H., Founti, M. A. and Markatos, N. C., "Modelling of Stretched Natural Gas Diffusion Flames", ***Applied Mathematical Modelling***, Vol. 24, Nos. 5-6, May (2000), 419-435.